
Cold-water coral habitats in the Penmarc'h and Guilvinec Canyons (Bay of Biscay): Deep-water versus shallow-water settings

Lies De Mol^{a,*}, David Van Rooij^a, Hans Pirlet^a, Jens Greinert^{a,b}, Norbert Frank^c,
Frédéric Quemmerais^{d,e}, Jean-Pierre Henriet^a

^a Renard Centre of Marine Geology (RCMG), Department of Geology and Soil Science, Ghent University, Krijgslaan 281 S8, B-9000 Gent, Belgium

^b Royal Netherlands Institute for Sea Research (NIOZ), P.O. Box 59, NL-1790 AB Den Burg, Texel, The Netherlands

^c Laboratoire des Sciences du Climat et de l'Environnement (LSCE), IPSL/CEA-CNRS-UVSQ, Bât.12, Avenue de la Terrasse, F-91190 Gif-sur-Yvette, France

^d Agence des aires marines protégées, 42 bis Quai de la Douane, BP 42932, F-29229 Brest Cedex 2, France

^e IFREMER, DEEP/LEP, BP 70, F-29280 Plouzané, France

*: Corresponding author : Lies De Mol, tel.: +32 9 264 46 37 ; fax: +32 9 264 49 67 ;
email address : Lies.DeMol@UGent.be

Abstract :

In 1948, Le Danois reported for the first time the occurrence of living cold-water coral reefs, the so-called "massifs coralliens", along the European Atlantic continental margin. In 2008, a cruise with R/V Belgica was set out to re-investigate these cold-water corals in the Penmarc'h and Guilvinec Canyons along the Gascogne margin of the Bay of Biscay. During this cruise, an area of 560 km² was studied using multibeam swath bathymetry, CTD casts, ROV observations and USBL-guided boxcoreing.

Based on the multibeam data and the ROV video imagery, two different cold-water coral reef settings were distinguished. In water depths ranging from 260 to 350 m, mini mounds up to 5 m high, covered by dead cold-water coral rubble, were observed. In between these mounds, soft sediment with a patchy distribution of gravel was recognised. The second setting (350–950 m) features hard substrates with cracks, spurs, cliffs and overhangs. In water depths of 700 to 950 m, both living and dead cold-water corals occur. Occasionally, they form dense coral patches with a diameter of about 10–60 m, characterised by mostly stacked dead coral rubble and a few living specimens. U/Th datings indicate a shift in cold-water coral growth after the Late Glacial Maximum (about 11.5 ka BP) from shallow to deep-water settings.

The living cold-water corals from the deeper area occur in a water density ($\sigma\text{-t}$) of 27.35–27.55 kg m⁻³, suggested to be a prerequisite for the growth and distribution of cold-water coral reefs along the northern Atlantic margin. In contrast, the dead cold-water coral fragments in the shallow area occur in a density range of 27.15–27.20 kg m⁻³ which is slightly outside the density range where living cold-water corals normally occur. The presented data suggest that this prerequisite is also valid for coral growth in the deeper canyons (> 350 m) in the Bay of Biscay.

Keywords : Bay of Biscay ; continental margin ; canyons ; cold-water corals ; *Lophelia* ; *Madrepora*

56 **1. Introduction**

57

58 Cold-water corals are widespread along the European Atlantic continental margin
59 (Freiwald and Roberts, 2005; Freiwald et al., 2004; Roberts et al., 2006, 2009). Previous
60 studies have already revealed a large amount of information about the distribution,
61 significance and environmental setting of these ecosystems along the Norwegian margin
62 (Fosså et al., 2005; Freiwald et al., 2002; Hovland et al., 1998; Lindberg and Mienert,
63 2005; Mortensen et al., 1995), and the continental margin off Ireland and the UK (De
64 Mol et al., 2002; Dorschel et al., 2007; Huvenne et al., 2007; Kenyon et al., 2003;
65 Masson et al., 2003; Mienis et al., 2007; Roberts et al., 2006; Van Weering et al., 2003;
66 Wheeler et al., 2007). Cold-water corals are able to form habitats which vary in size
67 from small patches (few metres in size) to large reef structures covering several
68 kilometres (Freiwald et al., 1999; Roberts et al., 2005). In the Porcupine Seabight and
69 Rockall Trough giant cold-water mounds up to 300 m high were observed (De Mol et
70 al., 2002; Kenyon et al., 2003; Wheeler et al., 2007; Van Weering et al., 2003). In
71 contrast to these well studied areas, coral occurrences within the Bay of Biscay, and
72 more specifically the Armorican margin, are less investigated (Reveillaud et al., 2008).

73

74 The occurrence of cold-water corals in the Bay of Biscay was already reported by
75 Joubin (1922) and Le Danois (1948). The latter study mainly observed the presence of
76 living *Madrepora oculata* and *Lophelia pertusa*, mostly occurring in a patchy
77 distribution but at some locations able to form a dense coral field with a maximum
78 height of 2 m. Afterwards these cold-water corals were also reported at different
79 locations in the Bay of Biscay by Altuna (1995), Alvarez-Claudio (1994), Zibrowius

80 (1980, 1985) and Zibrowius et al. (1975). In 1997, two areas along the north Atlantic
81 margin in the Bay of Biscay were revisited by Freiwald and Henrich (1997), namely the
82 Penmarc'h Bank and the Banc de la Chapelle, 160 km northwest of Penmarc'h Bank.
83 On the Banc de la Chapelle, only dead colonies of *Lophelia pertusa*, *Madrepora oculata*
84 and *Desmophyllum dianthus* were found in water depths of 340 to 790 m. Further south,
85 on the Penmarc'h Bank living colonies of *Dendrophyllia cornigera* were observed
86 (Reveillaud et al., 2008). The same authors also observed *Caryophyllia smithii*
87 specimens which yielded calibrated U/Th ages of the end of the last glacial period (11-
88 14 ka BP) (Schröder-Ritzrau et al., 2005). In 2008, Reveillaud et al. presented an
89 overview of the cold-water coral distribution and diversity in the Bay of Biscay based
90 on historical reports and more recent (pre-2008) data. However, it is still not known to
91 which extent the available information represents the actual distribution of cold-water
92 corals in the Bay of Biscay.

93

94 Cold-water corals occur in temperatures ranging between 4° and 12°C. This temperature
95 zone corresponds with water depths between ~50 and 1000 m at high latitudes and up to
96 4000 m at low latitudes (Freiwald et al., 2004). Besides temperature several other
97 environmental factors favour coral settlement and growth: hard substrates (e.g.,
98 boulders, moraine ridges, flanks of oceanic banks, seamounts, sedimentary mounds;
99 Dodge and Vaisnys, 1977; Rogers, 1990), strong topographically guided bottom
100 currents (Freiwald et al., 2004), nutrient-rich waters containing labile organic matter
101 (Kiriakoulakis et al., 2004) and zooplankton (Freiwald et al., 2004), and the depth of the
102 aragonite saturation horizon (Davies et al., 2008). Due to the presence of these
103 conditions along the continental slope in the Bay of Biscay, this area is a potential

104 habitat for cold-water coral ecosystems (Hall-Spencer et al., 2007; Reveillaud et al.,
105 2008). The numerous canyons cutting the slope of the Bay of Biscay (Bourillet et al.,
106 2003, 2006b; Le Suavé et al., 2000; Zaragosi et al., 2006) funnel sediment and labile
107 organic matter from the continental shelf (~200 m) to the abyssal plain (~4000 m)
108 (Freiwald et al., 2004). An additional major food source is provided by nutrient-rich
109 waters (Freiwald et al., 2004). Recently, Dullo et al. (2008) discovered that water
110 density also plays an important role in the distribution of cold-water corals. Along a
111 transect stretching from 51 to 70°N (~3000 km), living cold-water corals (*Lophelia*
112 *pertusa*) occur within a narrow density (sigma-theta) range of $\sigma_{\theta} = 27.35$ to 27.65 kg m^{-3} ,
113 independent from the surrounding water masses.

114

115 The data presented in this paper were collected during the BiSCOSYSTEMS cruise on
116 board of the R/V Belgica from 25 May to 7 June 2008 within the framework of the EC
117 FP6 IP HERMES and the ESF EuroDIVERSITY MiCROSYSTEMS projects. The main
118 aim of the study was (1) to revisit one of the cold-water coral locations described by Le
119 Danois (1948) in order to better understand their significance, distribution and
120 environmental conditions, and (2) to test the hypothesis that cold-water corals only
121 occur within the potential density range described by Dullo et al. (2008), also south of
122 51°N.

123

124 **2. Regional setting**

125

126 The continental margin in the Bay of Biscay can be subdivided in five main geographic
127 areas (Fig.1A): the Celtic margin and Armorican margin in the north, and the Aquitaine

128 margin, Cantabrian margin and Galician margin in the south. The Armorican margin
129 has an orientation of 140° with a relatively broad continental shelf, up to 200 km wide,
130 and a steep slope, with an average gradient between 2.86° and 5.15° (Lallemand and
131 Sibuet, 1986; Le Suavé et al., 2000). The slope extends from a water depth of 200 m
132 down to 4000 m. The morphology of the continental slope is characterised by spurs and
133 canyons, organised in submarine drainage basins (Bourillet and Lericolais, 2003).

134

135 The water column stratification in the Bay of Biscay predominantly shows that water
136 masses are of North Atlantic origin (Pollard et al., 1996). The uppermost water mass is
137 the Eastern North Atlantic Central Water (ENACW) which extends down to water
138 depths of 600 m. The ENACW is characterised by a cyclonic gyre with an average
139 velocity of 4 cm.s^{-1} (Pingree and Le Cann, 1989). Below a minimal density layer,
140 probably due to the influence of the Sub Antarctic Intermediate Water (SAIW), the
141 Mediterranean Outflow Water (MOW) is observed down to 1500 m water depth. Its
142 circulation as a contour current is conditioned by seafloor irregularities and the Coriolis
143 effect. MOW velocities have been measured in the Bay of Biscay at 8°W and 6°W with
144 average values of $2\text{-}3 \text{ cm.s}^{-1}$ (Pingree and Le Cann, 1989). Between 1500 and 3000 m
145 water depth, the North Atlantic Deep Water (NADW) is observed. It includes a core of
146 Labrador Sea Water (LSW), recognised by a salinity minimum at 1800 to 2000 m, and
147 the Iceland-Scotland Overflow Water (ISOW) which is identified by a small salinity
148 maximum around 2600 m (González-Pola, 2006; McCartney, 1992; McCave et al.,
149 2001; Pingree, 1973). Below the NADW, the Lower Deep Water (LDW) is identified
150 (McCartney, 1992). A cyclonic recirculation cell over the Biscay Abyssal Plain is

151 recognised with a characteristic poleward velocity near the continental margin of $1.2 (\pm$
152 $1.0) \text{ cm.s}^{-1}$ (Dickson et al., 1985; Paillet and Mercier, 1997).

153

154 Along the slopes of the Bay of Biscay strong, localised internal tides are reported, due
155 to a combination of favourable water mass stratification, steep topography and strong
156 barotropic tidal currents (Huthnance, 1995; Pingree and Le Cann, 1989, 1990). These
157 may be channelled and result in regions of locally increased flow and local circulations
158 (Pingree and Le Cann, 1990). Internal tides are proposed to explain the enhanced levels
159 of surface phytoplankton abundance (Holligan et al., 1985; Pingree and Griffiths, 1982).

160

161 **3. Materials and methods**

162

163 *3.1. Multibeam echosounding*

164

165 The multibeam echosounder used during the BiSCOSYSTEMS cruise is a Kongsberg
166 Simrad EM1002 system, installed permanently on the R/V Belgica. The EM1002 has up
167 to 111 receiver beams of 2° (across track) x 3.3° (along track) width. The high-
168 resolution depth data was obtained with a nominal frequency of 95 kHz and a ping-rate
169 of 4 to 6 Hz. Survey speed was between 4 and 6 knots depending on water depth and
170 wave conditions. In total, an area of 560 km² along the Armorican margin was mapped
171 in water depths between 160 m and 1000 m (Fig.1B).

172

173 The bathymetric information of the recorded files was extracted as xyz-data with the
174 open source MB-Systems software (Caress and Chayes, 1995). Next, data editing

175 occurred in the IVS Fledermaus software package resulting in a digital terrain model
176 (DTM) with a 5-m grid resolution.

177

178 *3.2. CTD measurements*

179

180 Two CTD casts (CTD 03: 46°51.990'N/5°31.768'W at 1450 m water depth and CTD
181 04: 46°54.536'N/5°21.262'W at 1250 m water depth) were obtained in the Guilvinec
182 Canyon using a SBE Seacat 19 in order to gain insight into the local water mass
183 stratification and to calibrate the EM1002 echosounder for sound velocity. The raw data
184 were binned at 1 m using the SBE Data Processing software (version 7.18c).

185

186 *3.3. ROV observations*

187

188 The Remotely Operated Vehicle (ROV) 'Genesis' from Ghent University is a Sub-
189 Atlantic Cherokee-type ROV with an operational survey depth down to 1600 m.
190 Imagery was obtained from one forward-looking colour camera, recorded with and
191 without a navigational overlay. High-resolution still images were obtained from a
192 Canon Powershot camera. Two parallel laser beams with a distance of 10 cm were used
193 as a scale during seabed observations. The ROV positioning was obtained using the
194 USBL (Ultra Short Base Line) IXSEA GAPS positioning system. This allowed
195 subsurface positioning with an accuracy of about 2-3 m. The processing and
196 interpretation of the dives was performed using OFOP (Ocean Floor Observation
197 Protocol) version 3.2.0c (Huetten and Greinert, 2008). Based on the observations, a

198 number of facies characteristic for the study area were identified. Each facies was given
199 a colour-code and integrated into ArcGIS 9.1, resulting in a facies interpretation map.

200

201 *3.4. Sedimentological analyses of boxcore samples*

202

203 Boxcores were taken at different locations within the Guilvinec Canyon. For each
204 boxcore, subsamples from different depths (mostly one sample from the surface and one
205 from the bottom) and/or subcores (if possible) were taken for sedimentological analysis.
206 Each subcore was sampled every 5 cm. The location of boxcores B08-1305-bc and B08-
207 1306-bc was accurately determined by using the GAPS USBL system.

208

209 Subsamples were analysed for grain-size distribution with a Malvern Mastersizer 2000
210 (Marine Biology Section, Ghent University). First, the sediment was dried in a furnace
211 at 60° for about 48h. After subsampling 1 cm³ of sediment, the carbonate fraction was
212 removed by adding 75 ml of 10% acetic acid (CH₃COOH). This process was performed
213 twice in order to remove all carbonate fragments. Afterwards, the sample was rinsed
214 twice with distilled water, each time followed by a 24 h settling period. Finally, the
215 sediment was transferred in a 15 ml centrifuge tube together with 0.2% calgon (sodium
216 hexametaphosphate, (NaPO₃)₆). Prior to analysis, the samples were rotated (20 rpm) for
217 24h. Afterwards, the results were processed with GRADISTAT (Blott and Pye, 2001)
218 and the mean grain-sizes were calculated using the Folk and Ward (1957) method.

219

220 Six cold-water coral specimens (*Lophelia pertusa*) from the surface of different
221 boxcores (B08-1301-bc, B08-1305-bc and B08-1306-bc) were sampled for U/Th dating.

222 The U-series measurements and age determination were carried out in the Laboratoire
223 des Sciences du Climat et de l'Environnement (LSCE) in Gif-sur-Yvette using
224 inductively coupled plasma source mass spectrometry (Thermo-Fisher X-Series).
225 Preparation of corals, analytical procedures and physical measurement routines
226 followed the detailed description by Frank et al. (2004, 2005) and Douville et al. (in
227 press).

228

229 **4. Results**

230

231 *4.1. Environmental setting of the canyons and spurs*

232

233 *4.1.1. Geomorphology*

234

235 The morphology of the canyon head and SE flank of the Penmarc'h Canyon, the
236 Guilvinec Canyon and the NW flank and canyon head of the Odet Canyon was studied
237 in detail using multibeam mapping (Fig.1B). These canyons are orientated in a NE-SW
238 direction and are separated by two spurs: the Penmarc'h Bank and the Odet Spur.

239

240 The Penmarc'h Canyon is a slightly asymmetric V-shaped canyon with a maximum
241 width of 10 km. The SE flank has an average slope of 10° and is incised by WNW-ESE
242 orientated gullies with average slopes varying between 9-14° (Fig. 1B).

243

244 The Guilvinec Canyon is an asymmetric V-shaped canyon with a maximum width of 16
245 km. The NW slope has an average slope of 8° whereas the SE slope is characterised by

246 an average slope of 6° . The total length of the canyon from the canyon head until the
247 abyssal plain is about 33 km and the maximum incision depth is 2 km. The slopes
248 flanking the canyons show ENE-WSW orientated gullies on the SE flanks with an
249 average slope of $8-11^\circ$ and NW-SE orientated gullies on the NW flanks with an average
250 slope of 10° . The width of the gullies varies between 600 and 1000 m.

251

252 The Odet Canyon is also an asymmetric V-shaped canyon with a maximum width of 9
253 km. The NW flank of the Odet Canyon has a constant average slope of about 11° ,
254 compared to the SE flank where an abrupt change in slope occurs around 1000 m water
255 depth. The NW slope of the Odet Canyon shows NW-SE orientated gullies with an
256 average slope of $8-12^\circ$.

257

258 The Penmarc'h Bank is a narrow spur with a minimum width of 4 km which goes up to
259 10 km close to the canyon heads. In contrast the Odet Spur has a maximum width of 14
260 km. Along both spurs, NE-SW orientated gullies occur with an average slope of $8-13^\circ$.
261 In the shallow area on the western part of the Odet Spur between 200 and 300 m water
262 depth, small mounds were observed with a diameter of approximately 100 m and a
263 height of 5 to 10 m.

264

265 *4.1.2. Hydrography*

266

267 The stratification of the water masses does not change significantly over the study area
268 (Fig. 2). The CTD casts show the presence of a seasonal thermocline down to 50 m
269 water depth. A salinity minimum (35.58 psu) is observed at 550 m, separating the

270 overlying ENACW from the MOW, which has its salinity maximum (35.76 psu) at
271 about 1000 m. Below, the T/S (temperature versus salinity) profile gradually follows the
272 27.75 kg.m^{-3} potential density gradient towards the LSW and NADW, as shown in
273 González-Pola (2006) and Van Rooij et al. (submitted-b).

274

275 4.2. Shallow-water coral rubble fields on Odet Spur

276

277 Mini mounds were observed on the multibeam echosounder data on Odet Spur in water
278 depths of 260 to 350 m. The gentle slope features an average gradient of 3-4° (Fig. 1B).
279 ROV observations allowed to distinguish four different facies: (1) rippled soft sediment
280 with a patchy distribution of dead cold-water corals (Fig. 3A), (2) rippled seabed with
281 biogenic debris and a patchy distribution of dead cold-water corals, (3) rippled soft
282 sediment covered with gravel or small pebbles (Fig. 3B), and (4) a dense cold-water
283 coral rubble coverage, dominated by *Lophelia pertusa* and/or *Madrepora oculata* (Fig.
284 3C and Fig. 3D).

285

286 Figure 4A shows that the small mounds are covered by dead cold-water coral rubble. At
287 the base of the mounds and in between them, an alternation of rippled soft sediment
288 with a patchy distribution of dead cold-water corals and/or biogenic debris, and rippled
289 soft sediment with gravel-sized particles was observed (Fig. 3A and Fig. 3B). The coral
290 rubble consists of crushed coral fragments (Fig. 3C and Fig. 3D) and nearly no visible
291 living fauna. The size of the coral rubble fields varies between 20 to 80 m. The
292 undulatory N-S to NNW-SSE orientated sand ripples appear with wavelengths between
293 5 and 10 cm and have heights of about 3-5 cm.

294

295 Boxcore samples were taken along the track of ROV dive B08-03 resulting in two
296 different lithofacies (Fig. 4B). Lithofacies 1 is characterised by olive brown to olive
297 grey poorly-sorted, fine to medium sand with mean grain-sizes varying between 215 μm
298 and 305 μm . Within this facies in boxcore B08-1302-bc fine laminations are observed
299 between olive brown and olive grey sand. In contrast, a clear colour change is observed
300 in boxcore B08-1305-bc at a depth of 5 cm. In boxcore B08-1303-bc, on top of a mini
301 mound (Fig. 4A), only a very thin layer of lithofacies 1 is observed. The surface of all
302 boxcores is covered with coarse biogenic debris and several *Lophelia pertusa* fragments
303 (1-4 cm), up to 5 cm depth. At the surface of boxcore B08-1303 also large gravel
304 fragments (up to 7 cm) were observed. Lithofacies 2 is characterised by olive grey very
305 poorly to poorly-sorted, medium silt with grain-sizes varying between 8.9 μm and 12.6
306 μm . Within this unit black sediment spots, supposedly caused by reducing geochemical
307 conditions, were observed. In boxcore B08-1303-bc a few sand lenses occur between 5
308 and 10 cm depth.

309

310 Boxcore B08-1304-bc had a penetration of only 5 cm (no subcoring). It consists of olive
311 grey, well sorted sand (lithofacies 1) with coarse biogenic debris and robust coral
312 fragments of *Lophelia pertusa* (several cm).

313

314 In addition, several coral fragments were dated using U-series: two coral fragments
315 (*Lophelia pertusa*) were collected during ROV dive B08-03, one coral fragment
316 (*Lophelia pertusa*) in boxcore B08-1301-bc and two coral fragments in B08-1305-bc.

317 The resulting ages after correction are shown in Table 3.

318

319 *4.3. Deep-water corals in the Penmarc'h and Guilvinec Canyons*

320

321 The second setting features cold-water corals observed in the Penmarc'h and Guilvinec
322 Canyons in water depths of 700 to 900 m. Both living and dead coral specimens occur,
323 predominantly *Madrepora oculata*. In total, eleven different facies were defined during
324 four ROV dives (Table 1). Facies 1 and 2 correspond to respectively even (Fig. 5A) and
325 rippled soft sediment with at some locations intense bioturbation. Facies 3 and 4
326 correspond to respectively even and rippled soft sediment covered with a patchy
327 distribution of cold-water corals (mostly *Madrepora oculata*) (Fig. 5B). Living as well
328 as dead species occur. Soft sediment with a cover of biogenic debris was defined as
329 facies 5 (Fig. 5C). No ripple marks were observed. Facies 6 and 7 are characterised by
330 respectively even and rippled soft sediment covered with biogenic debris and a patchy
331 distribution of cold-water corals (dead and living *Madrepora oculata*). Next, facies 8
332 consists of soft sediment with gravel (Fig. 5D). The gravel fragments reach sizes up to
333 10 cm. Facies 9 corresponds with outcropping hard substratum (Fig. 5E and Fig. 5F),
334 colonised by living cold-water corals (*Madrepora oculata*) and sponges. At some
335 locations, cracks filled with soft sediment were observed (Fig. 5G and Fig. 5H). Finally,
336 facies 10 and 11 relate to the cold-water coral coverage. Facies 10 is characterised by a
337 dense coverage of coral rubble (Fig. 6A) whereas facies 11 also features living species
338 of *Madrepora oculata* and *Lophelia pertusa* on top of the coral rubble, creating dense
339 coral fields (Fig. 6B, Fig. 6C and Fig. 6D). Facies 11 often coincides with a very rough
340 seafloor and big boulders (20 cm up to 1 m). Boxcore B08-1306-bc was taken within

341 this facies which delivered three coral pieces for U-series dating (Table 3). Grain-size
342 analysis reveals very poorly sorted fine sand with a mean grain-size of 81 μm .
343
344 Four ROV dives were undertaken. Dive B08-01 is located on the SE flank of the
345 Penmarc'h Canyon in water depths of 385 to 750 m. During this dive, an E-W
346 downslope transect was made with an average slope gradient of 8-10°. A large part of
347 the track consists of soft sediment with gravel (facies 8). At a water depth of 530 m the
348 gravel disappears and strongly bioturbated soft sediment (facies 1) remains until a water
349 depth of 720 m (Fig. 5A). Below 720 m, the first cold-water corals (facies 3) (*Lophelia*
350 *pertusa* and *Madrepora oculata*), with a size of 10-20 cm width and about 15 cm high,
351 appear on boulders with a diameter of 25 cm. Except for one living *Madrepora oculata*,
352 all corals are dead.
353
354 Dive B08-02 on the NW flank of the Guilvinec Canyon has a U-shaped track starting
355 with a first transect southwards from the NE flank of a gully at 712 m water depth and
356 ending with a second transect on the SW flank of that gully. The slope of this part
357 features an average gradient of 11°. During this dive many different facies were
358 observed (Fig. 7). In the uppermost part of the slope, between 700 and 900 m, soft
359 sediment alternates with coral fields which vary in diameter between 10 and 60 m (Fig.
360 6B). The soft sediment is sometimes covered with biogenic debris (Fig. 5C), gravel
361 (Fig. 5D) and/or a patchy distribution of cold-water corals, mostly *Madrepora oculata*.
362 Also big boulders with a diameter up to 1 m were observed, colonised with living cold-
363 water corals (*Madrepora oculata*) and *Hexadella sp.* sponges (Fig. 6E and Fig. 6F).
364 Between 800 and 900 m, asymmetric N-S orientated sand ripples appear with

365 wavelengths between 10 and 20 cm and with heights of about 5 cm. Below 900 m water
366 depth, mostly hard substratum (Fig. 5E and Fig. 5F) occurs with a patchy distribution of
367 living cold-water corals (*Madrepora oculata*). NW-SE orientated cracks of 5 cm up to
368 40 cm occur in this area, and are filled with (rippled) soft sediment (Fig. 5G and Fig.
369 5H). At several locations, the rather smoothly sloping seabed is interrupted by the
370 presence of small banks (Fig. 6G) or cliffs (Fig. 6H). Between 700 and 750 m water
371 depth, these escarpments have an E-W orientation, while the deeper ones reveal a S-N
372 or SSW-NNE orientation. The banks are generally few decimetres in height and thus
373 much smaller than the cliffs, which vary in height between 2 and 4 m. At three
374 locations, the escarpments are colonised by *Madrepora oculata* corals and
375 *Neopycnodonte zibrowii* oysters, which are discussed in more detail in Van Rooij et al.
376 (submitted-a).

377

378 Dive B08-04 is located on a small spur with dimensions of 200 by 400 m on the SE
379 flank of the Guilvinec Canyon in water depths of 675 to 700 m. Only one facies was
380 recognised: a dense cold-water coral coverage with dead and living species,
381 predominantly *Madrepora oculata* (Fig. 6C and Fig. 6D). The living species grow on
382 the dead coral rubble, which is built up by chunky coral fragments up to 40 cm.

383

384 Finally, dive B08-05 investigated the southern shoulder of a gully south of the spur that
385 separates the Penmarc'h Canyon from the Guilvinec Canyon. The track follows a
386 southern to western course between 300 and 750 m water depth with an overall slope
387 gradient of 8-10°. This track does not show many different facies. Between 300 and 450
388 m a rippled seafloor with regionally some biogenic debris and/or gravel was observed.

389 The straight to gently undulatory SSE-NNW orientated sand ripples have a wavelength
390 between 10 and 15 cm. The area between 450 and 730 m is characterised by soft
391 sediment with bioturbations and a zone of low-relief rippled seabed. Close to a water
392 depth of 480 m, some small escarpments are present. At 735 m, the gently dipping
393 seafloor is interrupted by a 4 m high WSW-ENE escarpment, colonised by *Madrepora*
394 *oculata* cold-water corals and *Neopycnodonte zibrowii* oysters (Van Rooij et al.,
395 submitted-a).

396

397 **5. Discussion**

398

399 *5.1. Canyons as cold-water coral habitats*

400

401 For the first time a cold-water coral habitat is mapped in detail within a canyon setting
402 in the Bay of Biscay. Although deep-sea canyons may provide suitable environmental
403 conditions for cold-water corals to grow, resulting deep-water habitats have not yet been
404 described in detail. Canyons are transport ways of organic matter from the continental
405 shelf down to the abyssal plain (Canals et al., 2006; Freiwald et al., 2004). During most
406 of the ROV dives described here, an intense marine snow was observed, composed of
407 suspended particulate material, ideal nutrients for scleractinians. In addition, the cold-
408 water corals occur just above, in case of the shallow water setting, and just beneath, in
409 case of the deep-water setting, the physical boundary between the Eastern North
410 Atlantic Central Water (ENACW) and the Mediterranean Outflow Water (MOW) (Fig.
411 2). As De Stigter et al. (2007) already demonstrated, the mixing of both water masses
412 results in enhanced suspended material thus favouring the feeding of scleractinians.

413 Moreover, the observations of ripple marks on the seabed, within the upper zone of the
414 MOW, indicate the presence of an E-W bottom current with a speed around 10 to 40
415 cm.s^{-1} (Stow et al., 2009). This elevated bottom current is beneficial for coral growth as
416 it delivers nutrients to the polyps. Additionally, the asymmetry of the sand ripples
417 shows a sediment transport direction away from the shelf edge into the canyon axis.
418 Similar observations were made by Cunningham et al. (2005) in the canyons on the
419 Celtic Margin between Goban Spur and Brenot Spur. Apart from the flow velocity of
420 the MOW, the bottom currents may be enhanced by strong internal tides (White, 2007).
421 Next to a favourable oceanographic environment, the sedimentological environment of
422 deep-sea canyons provides hard substrates for living cold-water corals to settle on.
423 Indeed, during the ROV dives, corals were observed on cliffs, outcropping hard
424 substratum and on the numerous boulders which are scattered on the seabed. The dives
425 also revealed a preferential erosion of the western flank of the canyons while the eastern
426 flank is draped with soft sediment. This is attributed to the strong E-W bottom currents.
427 The western slope will act as an obstacle for these enhanced currents intensifying the
428 easterly bottom currents through isopycnal doming, which results in erosion
429 (Hernandez-Molina et al., 2003; Iorga and Lozier, 1999; Van Rooij et al., submitted-a).
430 Hence, the constant reworking by downslope (turbiditic) and alongslope (contouritic)
431 current processes (Arzola et al., 2008; Bourillet et al., 2006b; Cunningham et al., 2005;
432 Pingree and Le Cann, 1989; Toucanne et al., 2009) which occur along this slope will
433 play an important role in the shaping of habitats suitable for coral settlement. This study
434 indicates that canyons are perfectly suited for coral growth due to the food availability,
435 strong bottom currents and the presence of hard substratum. More coral habitats might
436 be discovered in a similar setting in the future.

437

438 *5.2. Mini mounds on Odet Spur*

439

440 The shallow area, located in water depths between 278 and 289 m, revealed a dense
441 coverage of dead cold-water coral fragments on top of mini mounds and small ridges
442 (Fig. 4A). Within the boxcores, cold-water coral fragments were only found in the
443 uppermost 5 cm which suggests that these mini mounds were present before the settling
444 of the cold-water corals. The fact that the boxcores only show a thin sand cover (1.5 cm)
445 on top of the mini mound while at the base of the mound the sand cover increases to 11
446 cm, these mini mounds and ridges are probably the result of selective erosion of the
447 clayey substrate due to strong bottom currents during interglacials and interstadials, as
448 observed by Øvrebø et al. (2006) offshore Ireland. This observation highlights the
449 importance of an elevated topography which acts as a template for coral settlement
450 (Freiwald et al., 2004; Roberts et al., 2006). The lack of coral fragments deeper in the
451 sediment of the mini mounds is a fundamental difference with the giant coral mounds
452 observed along the Irish margin which are completely constructed by corals (Kano et
453 al., 2007). In that aspect, the mini mounds on Odet Spur reveal strong similarities with
454 the Darwin mounds in the northern Rockall Trough. The size of the coral topped
455 Darwin mounds is similar (height: 5 m / diameter: 75 m) but they are located in a deeper
456 water depth (1000 m). Coring revealed that corals are not a major contributor to mound
457 building (Masson et al., 2003). The Moira mounds in the Porcupine Seabight which are
458 characterised by diameters of 30-50 m and heights up to 5 m (Foubert et al., 2005;
459 Wheeler et al., 2005) might also serve as an analogue for the mounds observed on Odet
460 Spur.

461

462 *5.3. Time and distribution of coral growth*

463

464 The dating of the cold-water corals using U-series reveals that coral growth in the study
465 area started at the beginning of the Holocene. The older age of the corals in the shallow
466 (7.4-9.1 ka) compared to the deeper setting (1.2-2.3 ka) indicates a migration of the
467 coral habitats towards greater water depths. Moreover, the fact that the corals observed
468 in the shallow water setting are heavily bio-eroded and disintegrated, demonstrates that
469 they are already exposed on the seabed for a significant amount of time. In contrast, the
470 corals in the deeper setting are much better preserved suggesting a younger age for these
471 species. The cause of the downslope migration of the corals is still uncertain. However,
472 the changing sea level, influencing labile organic matter fluxes (Hall and McCave,
473 1998), and the rising temperatures, might have forced corals to deeper water depths,
474 where they found better live conditions. A more dramatic hypothesis is that the shallow
475 coral reefs were destroyed by bottom trawling since the shallower area is subject to
476 intense fishing activity (Bourillet et al., 2006a). According to Hily et al. (2008), a great
477 change has been observed in the benthic communities in the northern part of the Bay of
478 Biscay since the 1960s due to bottom trawling. Bottom trawling could also explain the
479 age difference between sample B08-03 C, with an age of 1.41 ± 0.17 ka, and the other
480 samples with ages over 7 ka (Table 3). Due to the reworking effect of trawling, most of
481 the coral reefs are turned upside down. However, no trawl marks were observed within
482 the shallow water area during the ROV dive.

483

484 On a more regional scale, the U-series datings of the corals confirm a climate-driven
485 influence. Since the Late Glacial Maximum (about 11.5 ka BP), extended living cold-
486 water coral reefs appear along the European margin between 50° and 70° N (Frank et
487 al., 2009). In contrast, during glacial times, the cold-water corals were only able to
488 survive in the relatively more temperate Atlantic below 50° N (Frank et al., submitted).
489 At present, only scarce coral occurrences are observed south of 50°N (Reveillaud et al.,
490 2008; Wienberg et al., 2009), which is also confirmed by the results presented in this
491 paper. The northern part of the Bay of Biscay, and more specifically the Armorican
492 margin, can be seen as a transition zone between the eastern temperate Atlantic and the
493 eastern North Atlantic between 50° and 70° N. This might explain why no successive
494 mound growth occurred in the Bay of Biscay, resulting in the build up of giant coral
495 mounds as discovered in the Porcupine Seabight (De Mol et al., 2002; Dorschel et al.,
496 2007; Henriët et al., 1998; Huvenne et al., 2007, 2009; Wheeler et al., 2005) and the
497 Rockall Trough (De Haas et al., 2009; Kenyon et al., 2003; Mienis et al., 2006; Van
498 Weering et al., 2003).

499

500 5.4. Relation between potential density and cold-water coral occurrence

501

502 The results of the present study may add to the theory of Dullo et al. (2008) who
503 concluded that the potential density (σ_{θ} = sigma-theta), where cold-water corals are
504 able to live and migrate along the Norwegian margin and in the Porcupine Seabight,
505 needs to be between 27.35 and 27.65 kg.m⁻³. The deeper canyon setting, where living
506 cold-water corals have been observed, is located in this density range (27.35 and 27.55
507 kg.m⁻³) (Fig.2) and thus supports the results of Dullo et al. (2008). In contrast, the dead

508 shallow water corals fall within a density range of 27.15-27.20 kg.m⁻³ which is slightly
509 outside the density range where living cold-water corals normally occur. This finding
510 demonstrates that the density range of 27.35 and 27.65 kg.m⁻³ is also valid for the living
511 cold-water corals in the Bay of Biscay. In addition, our results confirm that this density
512 range is not only applicable for dense living *Lophelia pertusa* reefs but also accounts in
513 this setting for living *Madrepora oculata* species.

514

515 **6. Conclusions**

516

517 Cold-water coral habitats along the Gascogne margin in the Bay of Biscay, earlier
518 reported by Le Danois in 1948, were investigated. The R/V Belgica BiSCOSYSTEMS
519 cruise was set out to better understand the significance and distribution of these cold-
520 water coral ecosystems and the environmental controls on their living habitat.

521

522 The main conclusions are:

- 523 • Deep-sea canyons such as the Penmarc'h and Guilvinec Canyons are suitable
524 habitats for the settlement of cold-water corals (*Madrepora oculata* and
525 *Lophelia pertusa*).
- 526 • Two cold-water coral settings were distinguished within the canyons: a shallow
527 setting in water depths of 280-290 m with only dead coral rubble (mostly
528 *Lophelia pertusa*) and a deep-water setting (700-920 m) with mostly living
529 *Madrepora oculata* species on top of coral rubble. The occurrence of the mini
530 mounds at ~280 m water depth is an unusually shallow water depth compared to
531 most other cold-water coral (reef) occurrences along the NE Atlantic margin.

- 532 • The Bay of Biscay can be considered as a transition zone between the temperate
533 Atlantic (below 50°N) and the cold north-eastern Atlantic between 50° and
534 70°N. After the Late Glacial Maximum, cold-water corals started to grow along
535 the Armorican margin but migrated likely during the mid Holocene to deeper
536 water depths.
- 537 • The density range of 27.35 to 27.65 kg.m⁻³ (Dullo et al., 2008) is also valid for
538 the living cold-water corals (mostly *Madrepora oculata*) in the Bay of Biscay,
539 which makes it a good prerequisite for the distribution and growth of living
540 cold-water corals along the northeast Atlantic margin. It can be used as a
541 predictive tool in order to discover more cold-water coral habitats along the
542 European continental margin.

543

544 **Acknowledgements**

545

546 The shipboard scientific party wants to thank the captain and crew of R/V Belgica for
547 their tremendous efforts and the fine cooperation during this campaign. This work was
548 financially supported by the the ESF EuroDIVERSITY project MiCROSYSTEMS
549 "Microbial diversity and functionality in cold-water coral reef ecosystems" and the EC
550 FP6 project HERMES (GOCE-CT-2005-511234-1) "Hotspot Ecosystem Research on
551 the Margins of European Seas", which will be continued during the FP7 HERMIONE
552 project (contract number 226354) "Hotspot Ecosystem Research and Man's Impact On
553 European Seas". We are grateful to Prof. Dr. M. Vincx (Marine Biology Department,
554 Ghent University) for allowing us to use the Malvern Mastersizer 2000. E. Sallé and C.
555 Noury from LSCE are kindly acknowledged for their help with respect to U series

556 sample preparation and dating. L. De Mol acknowledges the support of the “Institute for
557 the Promotion of Innovation through Science and Technology in Flanders (IWT-
558 Vlaanderen)”. H. Pirlet and D. Van Rooij are funded through respectively an FWO-
559 Flanders PhD and post-doctoral fellowship.

560

561 **References**

562

563 Altuna, A., 1995. El orden Scleractinia (Cnidaria, Anthozoa) en la costa vasca (Golfo de
564 Vizcaya): especies batiales de la fosa de CapBreton. *Munibe* 47, 85–96.

565 Alvarez-Claudio, C., 1994. Deep-water Scleractinia (Cnidaria: Anthozoa) from southern
566 Bay of Biscay. *Les Cahiers de Biologie Marine* 35, 461–469.

567 Arzola, R.G., Wynn, R.B., Lastras, G., Masson, D.G., Weaver, P.P.E., 2008.

568 Sedimentary features and processes in the Nazaré and Sétubal submarine
569 canyons, west Iberian margin. *Marine Geology* 250, 64-88.

570 Blott, S.J., Pye, K., 2001. Gradistat: a grain size distribution and statistics package for
571 the analysis of unconsolidated sediments. *Earth Surface Processes and*
572 *Landforms* 26, 1237-1248.

573 Bourillet, J.-F., Lericolais, G., 2003. Morphology and seismic stratigraphy of the
574 Manche Paleoriver System, Western Approaches, in: Mienert, J., Weaver, P.
575 (Eds.), *European Margin Sediment Dynamics*, Springer, Verlag Berlin
576 Heidelberg, pp. 229-233.

577 Bourillet, J.-F., Reynaud, J.-Y., Baltzer, A., Zaragosi, S., 2003. The 'Fleuve Manche':
578 the submarine sedimentary features from the outer shelf to the deep-sea fans.
579 *Journal of Quaternary Science* 18 (3-4), 261-282.

580 Bourillet, J.F., Jouanneau, J.-M., Macher, C., Le Hir, P., Naughton, F., 2006a. "La
581 Grande Vasière" mid-shelf mud belt: Holocene sedimentary structure, natural
582 and anthropogenic impacts. 10th International Symposium on Oceanography of
583 the Bay of Biscay, Vigo, Spain.

584 Bourillet, J.-F., Zaragosi, S., Mulder, T., 2006b. The French Atlantic margin and deep-
585 sea submarine systems. *Geo-Marine Letters* 26, 311-315.

586 Canals, M., Puig, P., Durrieu de Madron, X., Heussner, S., Palanques, A., Fabres, J.,
587 2006. Flushing submarine canyons. *Nature* 444, 354-357.

588 Caress, D.W., Chayes, D.N., 1995. New software for processing sidescan data from
589 sidescan-capable multibeam sonars, in: Wernli, R. (Ed.), *Oceans 95 MTS/IEEE:
590 Challenges of our Changing Global Environment, Conference Proceedings*, vol.
591 2, Marine Technology Society Journal, Washington DC, pp. 997-1000.

592 Cunningham, M.J., Hodgson, S., Masson, D.G., Parson, L.M., 2005. An evaluation of
593 along- and down-slope sediment transport processes between Goban Spur and
594 Brenot Spur on the Celtic Margin of the Bay of Biscay. *Sedimentary Geology*
595 179, 99-116.

596 Davies, A.J., Wisshak, M., Orr, J.C., Roberts, J.M., 2008. Predicting suitable habitat for
597 the cold-water coral *Lophelia pertusa* (Scleractinia). *Deep-Sea Research I* 55,
598 1048-1062.

599 De Haas, H., Mienis, F., Frank, N., Richter, T.O., Steinacher, R., de Stigter, H., van der
600 Land, C., van Weering, T.C.E., 2009. Morphology and sedimentology of
601 (clustered) cold-water coral mounds at the south Rockall Trough margins, NE
602 Atlantic Ocean. *Facies* 55, 1-26.

603 De Mol, B., Van Rensbergen, P., Pillen, S., Van Herreweghe, K., Van Rooij, D.,
604 McDonnell, A., Huvenne, V., Ivanov, M., Swennen, R., Henriët, J.-P., 2002.
605 Large deep-water coral banks in the Porcupine Basin, southwest of Ireland.
606 *Marine Geology* 188, 193-231.

607 De Stigter, H., Boer, W., Mendes, P.A.D.J., Jesus, C.C., Thomsen, L., van den Bergh,
608 G.D., van Weering, T.C.E., 2007. Recent sediment transport and deposition in
609 the Nazaré Canyon, Portuguese continental margin. *Marine Geology* 246, 144-
610 164.

611 Dickson, R.R., Gould, W.J., Muller, T.J., Maillard, C., 1985. Estimates of the mean
612 circulation in the deep (> 2000 m) layer of the eastern North Atlantic. *Progress*
613 *in Oceanography* 14, 103-127.

614 Dodge, R.E., Vaisnys, J.R., 1977. Coral populations and growth patterns: responses to
615 sedimentation and turbidity associated with dredging. *Journal of Marine*
616 *Research* 35, 715-730.

617 Dorschel, B., Hebbeln, D., Foubert, A., White, M., Wheeler, A.J., 2007.
618 Hydrodynamics and cold-water coral facies distribution related to recent
619 sedimentary processes at Galway Mound west of Ireland. *Marine Geology* 244,
620 184-195.

621 Douville, E., Sallé, E., Frank, N., Eisele, M., Pons-Branchu, E., Ayrault, S., in press.
622 Rapid and accurate U-Th dating of ancient carbonates using inductively coupled
623 plasma-quadrupole mass spectrometry. *Chemical Geology*, doi:
624 10.1016/j.chemgeo.2010.01.007.

625 Dullo, W.-C., Flögel, S., Rüggeberg, A., 2008. Cold-water coral growth in relation to
626 the hydrography of the Celtic and Nordic European continental margin. *Marine*
627 *Ecology Progress Series* 371, 165-176.

628 Folk, R.L., Ward, W., 1957. Brazos River bar: a study in the significance of grain size
629 parameters. *Journal of Sedimentary Petrology* 27, 3-26.

630 Fosså, J.H., Lindberg, B., Christensen, O., Lundälv, T., Svellingen, I., Mortensen, P.B.,
631 Alvsvåg, J., 2005. Mapping of *Lophelia* reefs in Norway: experiences and
632 survey methods, in: Freiwald, A., Roberts, J.M. (Eds.), *Cold-water corals and*
633 *ecosystems*, Springer, Heidelberg, pp. 359-390.

634 Foubert, A., Beck, T., Wheeler, A.J., Opderbecke, J., Grehan, A., Klages, M., Thiede,
635 J., Henriët, J.-P., the Polarstern ARK-XIX/3a Shipboard Party, 2005. New view
636 of the Belgica Mounds, Porcupine Seabight, NE Atlantic: preliminary results
637 from the Polarstern ARK-XIX/3a ROV cruise, in: Freiwald, A., Roberts, J.M.
638 (Eds.), *Cold-Water Corals and Ecosystems*, Springer, Heidelberg, pp. 403-415.

639 Frank, N., Freiwald, A., López-Correa, M., Eisele, M., Hebbeln, D., Wienberg, C., Van
640 Rooij, D., Henriët, J.-P., Colin, C., van Weering, T., de Haas, H., Mortensen,
641 P.B., Robberts, M., De Mol, B., Douville, E., Blamart, D., Hatte, C., submitted.
642 Climate warming drives eastern Atlantic cold-water coral gardens northwards.
643 *Nature Geoscience*.

644 Frank, N., Lutringer, A., Paterne, M., Blamart, D., Henriët, J.-P., Van Rooij, D., van
645 Weering, T.C.E., 2005. Deep-water corals of the northeastern Atlantic margin:
646 carbonate mound evolution and upper intermediate water ventilation during the
647 Holocene, in: Freiwald, A., Roberts, J.M. (Eds.), *Cold-Water Corals and*
648 *Ecosystems*, Springer, Heidelberg, pp. 113-133.

649 Frank, N., Paterne, M., Ayliffe, L., van Weering, T.C.E., Henriët, J.-P., Blamart, D.,
650 2004. Eastern North Atlantic deep-sea corals: Tracing upper intermediate water
651 $\delta^{14}\text{C}$ during the Holocene. *Earth and Planetary Science Letters* 219, 297-309.

652 Frank, N., Ricard, E., Lutringer-Paquet, A., van der Land, C., Colin, C., Blamart, D.,
653 Foubert, A., Van Rooij, D., Henriët, J.-P., de Haas, H., van Weering, T., 2009.
654 The Holocene occurrence of cold water corals in the NE Atlantic: Implications
655 for coral carbonate mound evolution. *Marine Geology* 266, 129-142.

656 Freiwald, A., Fosså, J.H., Grehan, A., Koslow, T., Roberts, J.M., 2004. Cold-water
657 coral reefs: out of sight, no longer out of mind. UNEP-WCMC, Cambridge, UK.
658 Biodiversity Series 22, 1-84.

659 Freiwald, A., Henrich, R., 1997. Victor Hensen Cruise VH-97 Leg 1 and Leg 5.
660 Unpublished report and station list. Institut für Paläontologie, Universität
661 Erlangen, Erlangen, Germany.

662 Freiwald, A., Hühnerbach, V., Lindberg, B., Wilson, J.B., Campbell, J., 2002. The Sula
663 Reef complex, Norwegian Shelf. *Facies* 47, 179-200.

664 Freiwald, A., Roberts, J.M., 2005. Cold-water corals and ecosystems. Springer,
665 Heidelberg.

666 Freiwald, A., Wilson, J.B., Henrich, R., 1999. Grounding Pleistocene icebergs shape
667 recent deep-water coral reefs. *Sedimentary Geology* 125, 1-8.

668 González-Pola, C., Lavin, A., Somavilla, R., Vargas-Yanez, M., 2006. Central water
669 masses variability in the southern Bay of Biscay from early 90s. The effect of
670 the severe winter 2005, in: ICES Annual Science Conference, Maastricht,
671 September 2006, C26, pp. 1–12.

672 Hall, I.R., McCave, I.N., 1998. Glacial-interglacial variation in organic carbon burial on
673 the slope of the N.W. European Continental Margin (48°-50°N). Progress in
674 Oceanography 42, 37-60.

675 Hall-Spencer, J., Rogers, A., Davies, J., Foggo, A., 2007. Deep-sea coral distribution on
676 seamounts, oceanic islands, and continental slopes in the Northeast Atlantic, in:
677 George, R.Y., Cairns, S.D. (Eds.), Conservation and Adaptive Management of
678 Seamount and Deep-Sea Coral Ecosystems, pp. 135-146.

679 Henriot, J.P., De Mol, B., Pillen, S., Vanneste, M., 1998. Gas hydrate crystals may help
680 build reefs. Nature 391, 648-649.

681 Hernández-Molina, F.J., Llave, E., Somoza, L., Fernandez-Puga, M.C., Maestro, A.,
682 Leon, R., Medialdea, T., Barnolas, A., Garcia, M., de Rio, V.D., Fernandez-
683 Salas, L.M., Vazquez, J.T., Lobo, F., Dias, J.M.A., Rodero, J., Gardner, J., 2003.
684 Looking for clues to paleoceanographic imprints: A diagnosis of the Gulf of
685 Cadiz contourite depositional systems. Geology 31 (1), 19-22.

686 Hily, C., Le Loc'h, F., Grall, J., Glémarec, M., 2008. Soft bottom macrobenthic
687 communities of North Biscay revisited: Long-term evolution under fisheries-
688 climate forcing. Estuarine, Coastal and Shelf Science 78, 413-425.

689 Holligan, P.M., Pingree, R.D., Mardell, G.T., 1985. Oceanic Solitions, Nutrient Pulses
690 and Phytoplankton Growth. Nature 314, 348-350.

691 Hovland, M., Mortensen, P.B., Brattegard, T., Strass, P., Rokoengen, K., 1998.
692 Ahermatypic coral banks off Mid-Norway: evidence for a link with seepage of
693 light hydrocarbons. Palaios 13, 189-200.

694 Huetten, E., Greinert, J., 2008. Software controlled guidance, recording and post-
695 processing of seafloor observations by ROV and other towed devices: The

696 software package OFOP. Geophysical Research Abstracts 10, EGU2008-A-
697 03088.

698 Huthnance, J.M., 1995. Circulation, exchange and water masses at the ocean margin:
699 the role of physical processes at the shelf edge. Progress in Oceanography 35,
700 353-431.

701 Huvenne, V.A.I., Bailey, W.R., Shannon, P.M., Naeth, J., de Primio, R., Henriët, J.P.,
702 Horsfield, B., de Haas, H., Wheeler, A., Olu-Le Roy, K., 2007. The Magellan
703 mound province in the Porcupine Basin. International Journal of Earth Sciences
704 96, 85-101.

705 Huvenne, V.A.I., Van Rooij, D., De Mol, B., Thierens, M., O'Donnell, R., Foubert, A.,
706 2009. Sediment dynamics and palaeo-environmental context at key stages in the
707 Challenger cold-water coral mound formation: Clues from sediment deposits at
708 the mound base. Deep-Sea Research I 56 (12), 2263-2280.

709 Iorga, M.C., Lozier, M.S., 1999. Signatures of the Mediterranean outflow from a North
710 Atlantic climatology 1. Salinity and density fields. Journal of Geophysical
711 Research - Oceans 104 (C11), 25985-26009.

712 Joubin, M.L., 1922. Les coraux de mer profonde nuisibles aux chalutiers. Note et
713 Mémoires N° 18, Office Scientifique et Technique des Pêches Maritimes, Paris.

714 Kano, A., Ferdelman, T.G., Williams, T., Henriët, J.P., Ishikawa, T., Kawagoe, N.,
715 Talkashima, C., Kakizaki, Y., Abe, K., Sabai, S., Browning, E.L., Li, X.H.,
716 Integrated Ocean Drilling Program, 2007. Age constraints on the origin and
717 growth history of a deep-water coral mound in the northeast Atlantic drilled
718 during Integrated Ocean Drilling Program Expedition 307. Geology 35 (11),
719 1051-1054.

720 Kenyon, N.H., Akhmetzhanov, A.M., Wheeler, A.J., van Weering, T.C.E., de Haas, H.,
721 Ivanov, M.K., 2003. Giant carbonate mud mounds in the southern Rockall
722 Trough. *Marine Geology* 195, 5-30.

723 Kiriakoulakis, K., Bett, B.J., White, M., Wolff, G.A., 2004. Organic biogeochemistry of
724 the Darwin Mounds, a deep-water coral ecosystem, of the NE Atlantic. *Deep-*
725 *Sea Research I* 51, 1937-1954.

726 Lallemand, S., Sibuet, J.C., 1986. Tectonic Implications of Canyon Directions over the
727 Northeast Atlantic Continental-Margin. *Tectonics* 5 (7), 1125-1143.

728 Le Danois, E., 1948. *Les profondeurs de la mer. Trente ans de recherche sur la faune*
729 *sous-marine au large des côtes de France.* Payot, Paris.

730 Le Suavé, R., Bourillet, J.F., Coutelle, A., 2000. *La marge nord du golfe de Gascogne.*
731 *Connaissances générales du rapport des nouvelles synthèses de données*
732 *multifaisceaux.* IFREMER, Paris.

733 Lindberg, B., Mienert, J., 2005. Post-glacial carbonate production by cold-water corals
734 on the Norwegian Shelf and their role in the global carbonate budget. *Geology*
735 33, 537-540.

736 Masson, D.G., Bett, B.J., Billett, D.S.M., Jacobs, C.L., Wheeler, A.J., Wynn, R.B.,
737 2003. The origin of deep-water, coral-topped mounds in the northern Rockall
738 Trough, Northeast Atlantic. *Marine Geology* 194 (3-4), 159-180.

739 McCartney, M.S., 1992. Recirculating components to the deep boundary current of the
740 northern North Atlantic. *Progress in Oceanography* 29, 283-383.

741 McCave, I.N., Hall, I.R., Antia, A.N., Chou, L., Dehairs, F., Lampitt, R.S., Thomsen,
742 L., van Weering, T.C.E., Wollast, R., 2001. Distribution, composition and flux

743 of particulate material over the European margin at 47°-50°N. Deep-Sea
744 Research II 48, 3107-3139.

745 Mienis, F., de Stigter, H.C., White, M., Duineveld, G., de Haas, H., van Weering,
746 T.C.E., 2007. Hydrodynamic controls on cold-water coral growth and carbonate-
747 mound development at the SW and SE Rockall Trough Margin, NE Atlantic
748 Ocean. Deep-Sea Research I 54, 1655-1674.

749 Mienis, F., van Weering, T.C.E., de Haas, H., de Stigter, H., Huvenne, V.A.I., Wheeler,
750 A., 2006. Carbonate mound development at the SW Rockall Trough margin
751 based on high resolution TOBI and seismic recording. Marine Geology 233, 1-9.

752 Mortensen, P.B., Hovland, M., Brattegard, T., Farestveit, R., 1995. Deep water
753 bioherms of the scleractinian coral *Lophelia pertusa* (L.) at 64°N on the
754 Norwegian shelf: structure and associated mega-fauna. Sarsia 80, 145-158.

755 Normand, A., Mazé, J.-P., 2000. Cartes bathymétriques au 1/250 000ème: Marge
756 celtique Est, Marge armoricaine Nord, Sud Trevelyan, Dôme Gascogne, Marge
757 armoricaine sud, Marge Aquitaine, in: Le Suavé, R. (Ed.), Synthèse
758 bathymétrique et imagerie acoustique, Zone Economique Exclusive Atlantique
759 Nord-Est, Editions IFREMER.

760 Øvrebø, L.K., Haughton, P.D.W., Shannon, P.M., 2006. A record of fluctuating bottom
761 currents on the slopes west of the Porcupine Bank, offshore Ireland –
762 implications for Late Quaternary climate forcing. Marine Geology 225 (1-4),
763 279-309.

764 Paillet, J., Mercier, H., 1997. An inverse model of the eastern North Atlantic general
765 circulation and thermocline ventilation. Deep-Sea Research I 44 (8), 1293-1328.

766 Pingree, R.D., 1973. Component of Labrador Sea-Water in Bay-of-Biscay. *Limnology*
767 *and Oceanography* 18 (5), 711-718.

768 Pingree, R.D., Griffiths, D.K., 1982. Tidal Friction and the Diurnal Tides on the
769 Northwest European Shelf. *Journal of the Marine Biological Association of the*
770 *United Kingdom* 62 (3), 577-593.

771 Pingree, R.D., Le Cann, B., 1989. Celtic and Armorican slope and shelf residual
772 currents. *Progress in Oceanography* 23, 303-338.

773 Pingree, R.D., Le Cann, B., 1990. Structure, strength and seasonality of the slope
774 currents in the Bay of Biscay region. *Journal of the Marine Biological*
775 *Association of the United Kingdom* 70, 857-885.

776 Pollard, S., Griffiths, C.R., Cunningham, S.A., Read, J.F., Perez, F.F., Ríos, A.F., 1996.
777 Vivaldi 1991 – A study of the formation, circulation and ventilation of the
778 Eastern North Atlantic Central Water. *Progress in Oceanography* 37, 167-192.

779 Reveillaud, J., Freiwald, A., Van Rooij, D., Le Guilloux, E., Altuna, A., Foubert, A.,
780 Vanreusel, A., Olu-Le Roy, K., Henriët, J.-P., 2008. The distribution of
781 scleractinian corals in the Bay of Biscay, NE Atlantic. *Facies* 54 (3), 317-331.

782 Roberts, J.M., Brown, C.J., Long, D., Bates, C.R., 2005. Acoustic mapping using a
783 multibeam echosounder reveals cold-water coral reefs and surrounding habitats.
784 *Coral Reefs* 24, 654-669.

785 Roberts, J.M., Wheeler, A.J., Freiwald, A., 2006. Reefs of the deep: the biology and
786 geology of cold-water coral ecosystems. *Science* 312, 543-546.

787 Roberts, J.M., Wheeler, A., Freiwald, A., Cairns, S., 2009. Cold-water corals – The
788 biology and geology of deep-sea coral habitats. Cambridge University Press.

- 789 Rogers, C.S., 1990. Responses of coral reefs and reef organisms to sedimentation.
790 Marine Ecology Progress Series 62, 184-202.
- 791 Schröder-Ritzrau, A., Freiwald, A., Mangini, A., 2005. U/Th dating of deep-water
792 corals from the eastern North Atlantic and the western Mediterranean Sea, in:
793 Freiwald, A., Roberts, J.M. (Eds.), Cold-water corals and ecosystems, Springer,
794 Heidelberg, pp. 157-172.
- 795 Stow, D.A.V., Hernandez-Molina, F.J., Llave, E., Sayago-Gil, M., del Rio, V.D.,
796 Branson, A., 2009. Bedform-velocity matrix: The estimation of bottom current
797 velocity from bedform observations. *Geology* 37 (4), 327-330.
- 798 Toucanne, S., Zaragosi, S., Bourillet, J.F., Cremer, M., Eynaud, F., Van Vliet-Lanoë,
799 B., Penaud, A., Fontanier, C., Turon, J.L., Cortijo, E., Gibbard, P.L., 2009.
800 Timing of massive 'Fleuve Manche' discharges over the last 350 kyr: insights
801 into the European ice-sheet oscillations and the European drainage network from
802 MIS 10 to 2. *Quaternary Science Reviews* 28 (13-14), 1238-1256.
- 803 Van Rooij, D., De Mol, L., Le Guilloux, E., Wisshak, M., Huvenne, V.A.I.,
804 Moeremans, R., Henriët, J.-P., submitted-a. Environmental setting of deep-water
805 oysters in the Bay of Biscay. *Deep-Sea Research I*.
- 806 Van Rooij, D., Iglesias, J., Hernandez-Molina, F.J., Ercilla, G., Gomez-Ballesteros, M.,
807 Casas, D., Llave, E., De Hauwere, A., Garcia-Gil, S., Acosta, J., Henrich, R.,
808 submitted-b. The Le Danois Contourite Depositional System: interactions
809 between the Mediterranean Outflow Water and the upper Cantabrian slope
810 (North Iberian Margin). *Marine Geology*.

811 Van Weering, T.C.E., de Haas, H., de Stigter, H.C., Lykke-Andersen, H., Kouvaev, I.,
812 2003. Structure and development of giant carbonate mounds at the SW and SE
813 Rockall Trough margins, NE Atlantic Ocean. *Marine Geology* 198 (1-2), 67-81.

814 Wheeler, A.J., Beyer, A., Freiwald, A., de Haas, H., Huvenne, V.A.I., Kozachenko, M.,
815 Olu-Le Roy, K., Opderbecke, J., 2007. Morphology and environment of cold-
816 water coral carbonate mounds on the NW European margin. *International*
817 *Journal of Earth Sciences* 96, 37-56.

818 Wheeler, A.J., Kozachenko, M., Beyer, A., Foubert, A., Huvenne, V.A.I., Klages, M.,
819 Masson, D.G., Olu-Le Roy, K., Thiede, J., 2005. Sedimentary processes and
820 carbonate mounds in the Belgica mound province, Porcupine Seabight, NE
821 Atlantic, in: Freiwald, A., Roberts, J.M. (Eds.), *Cold-Water Corals and*
822 *Ecosystems*, Springer, Heidelberg, pp. 571-603.

823 White, M., 2007. Benthic dynamics at the carbonate mound regions of the Porcupine
824 Sea Bight continental margin. *International Journal of Earth Sciences* 96, 1-9.

825 Wienberg, C., Hebbeln, D., Fink, H.G., Mienis, F., Dorschel, B., Vertino, A., López
826 Correa, M., Freiwald, A., 2009. Scleractinian cold-water corals in the Gulf of
827 Cádiz – First clues about their spatial and temporal distribution. *Deep-Sea*
828 *Research I* 156, 1873-1893.

829 Zaragosi, S., Bourillet, J.-F., Eynaud, F., Toucanne, S., Denhard, B., Van Toer, A.,
830 Lanfumey, V., 2006. The impact of the last European deglaciation on the deep-
831 sea turbidite systems of the Celtic-Armorican margin (Bay of Biscay). *Geo-*
832 *Marine Letters* 26, 317-329.

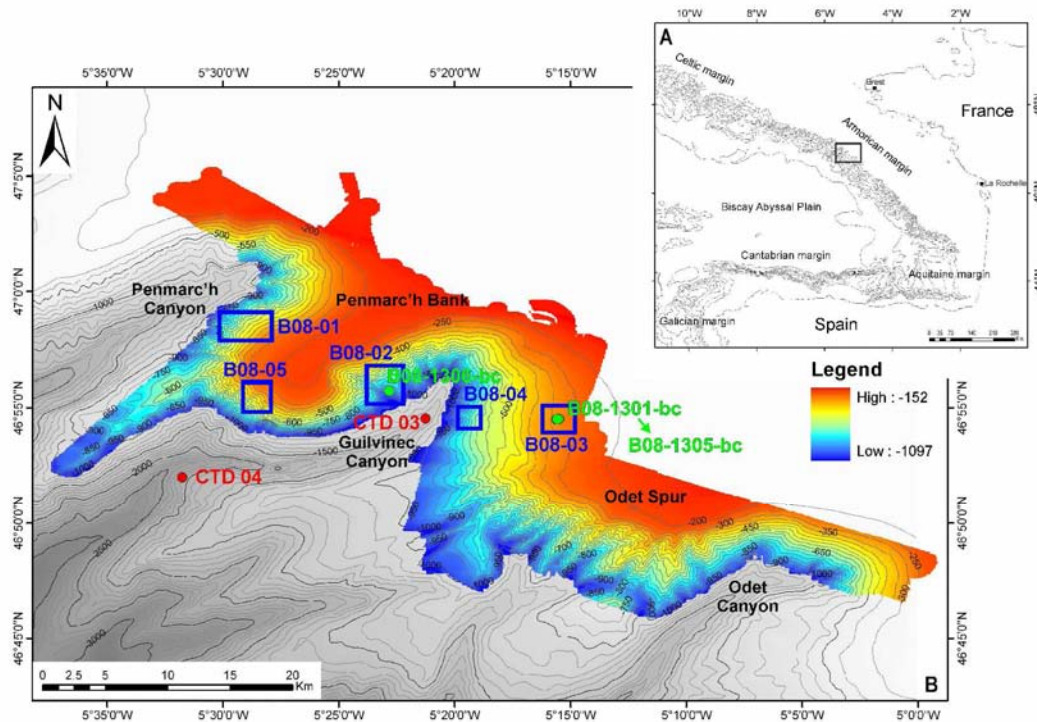
833 Zibrowius, H., 1980. Les Scléactiniales de la Méditerranée et de l'Atlantique nord-
834 oriental. *Mémoires de l'Institut Océanographique Monaco* 11, 1-284.

- 835 Zibrowius, H., 1985. Scléactiniaires bathyaux et abyssaux de l'Atlantique nord-
836 oriental: campagnes BIOGAS (POLGAS) et INCAL, in: Laubier, L., Monniot,
837 C. (Eds.), Peuplements profonds du Golfe de Gascogne, IFREMER, Brest,
838 France, pp. 311–324.
- 839 Zibrowius, H., Southward, E.C., Day, J.H., 1975. New observations on a little-known
840 species of *Lumbrineris* (Polychaeta) living on various cnidarians, with notes on
841 its recent and fossil scleractinian hosts. *Journal of the Marine Biological*
842 *Association of the United Kingdom* 55, 83–108.

843 **Figures**

844

845 Figure 1.



846

847 (A) Location of the study area along the French Atlantic continental margin (GEBCO

848 bathymetry, contour lines every 500 m), (B) Detail of the study area with EM1002

849 bathymetry (contour lines every 50 m) and the location of the CTD casts (red), ROV

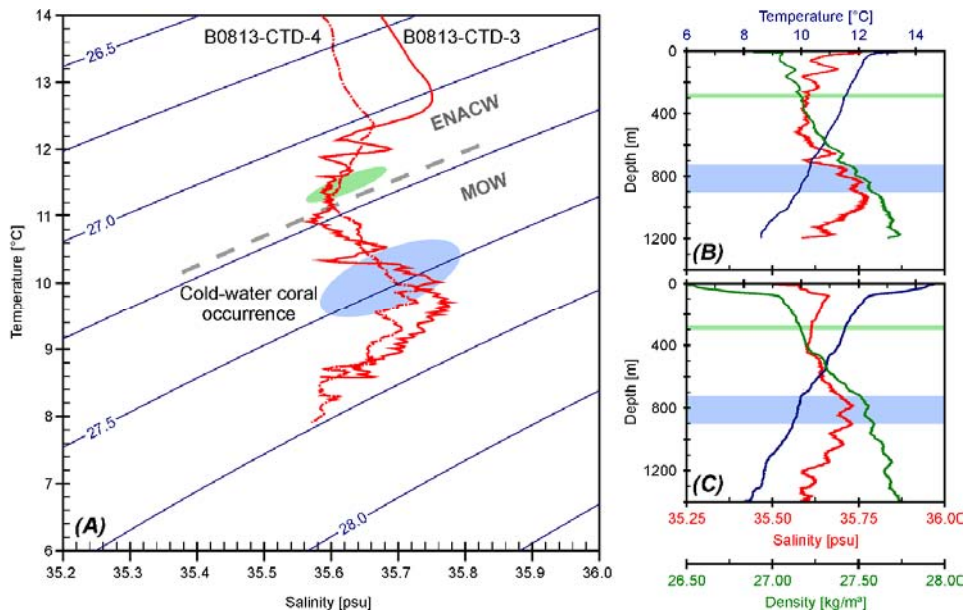
850 dives (blue) and boxcores (green), collected during the R/V Belgica BiSCOSYSTEMS

851 cruise (2008). As background a bathymetric map of IFREMER (Normand and Mazé,

852 2000) is used (contour lines every 100 m).

853

854 Figure 2.

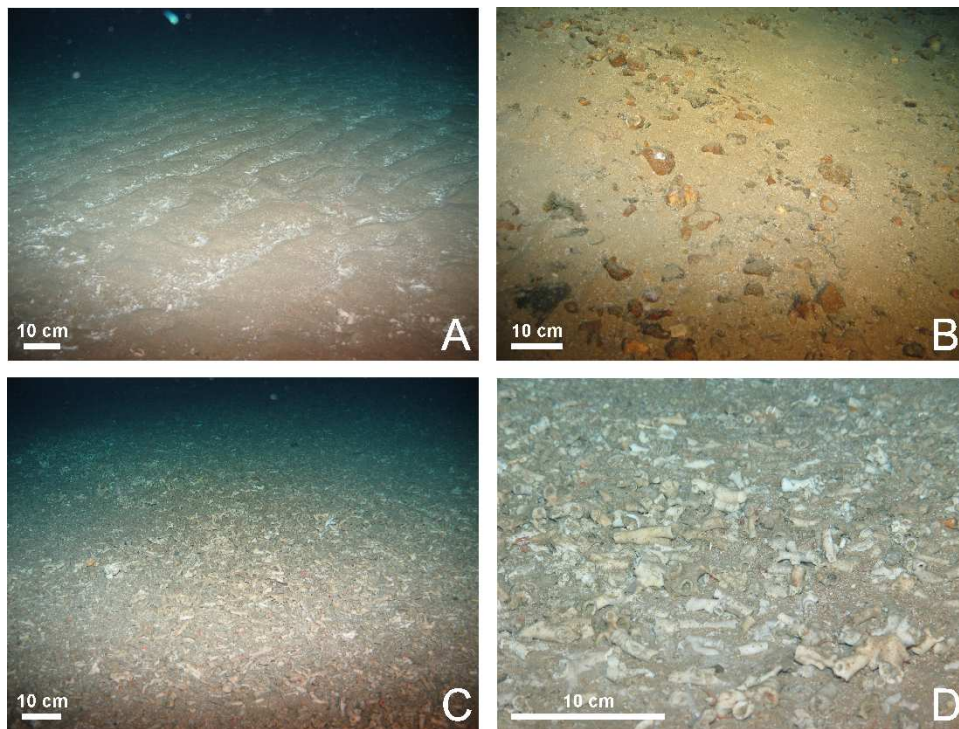


855

856 Hydrographic data of the Guilvinec Canyon. (A) Temperature/salinity plot for both
857 CTD casts, with indication of the boundary (dashed grey line) between the Eastern
858 North Atlantic Central Water (ENACW) and the Mediterranean Outflow Water
859 (MOW). The estimated occurrence envelope of the shallow-water (green) and deep-
860 water (blue) cold-water corals in the Penmarc'h and Guilvinec Canyons is based on the
861 ROV observations, plotted on the CTD data of respectively (B) cast B0813-CTD-3 and
862 (C) cast B0813-CTD-4.

863

864 Figure 3.

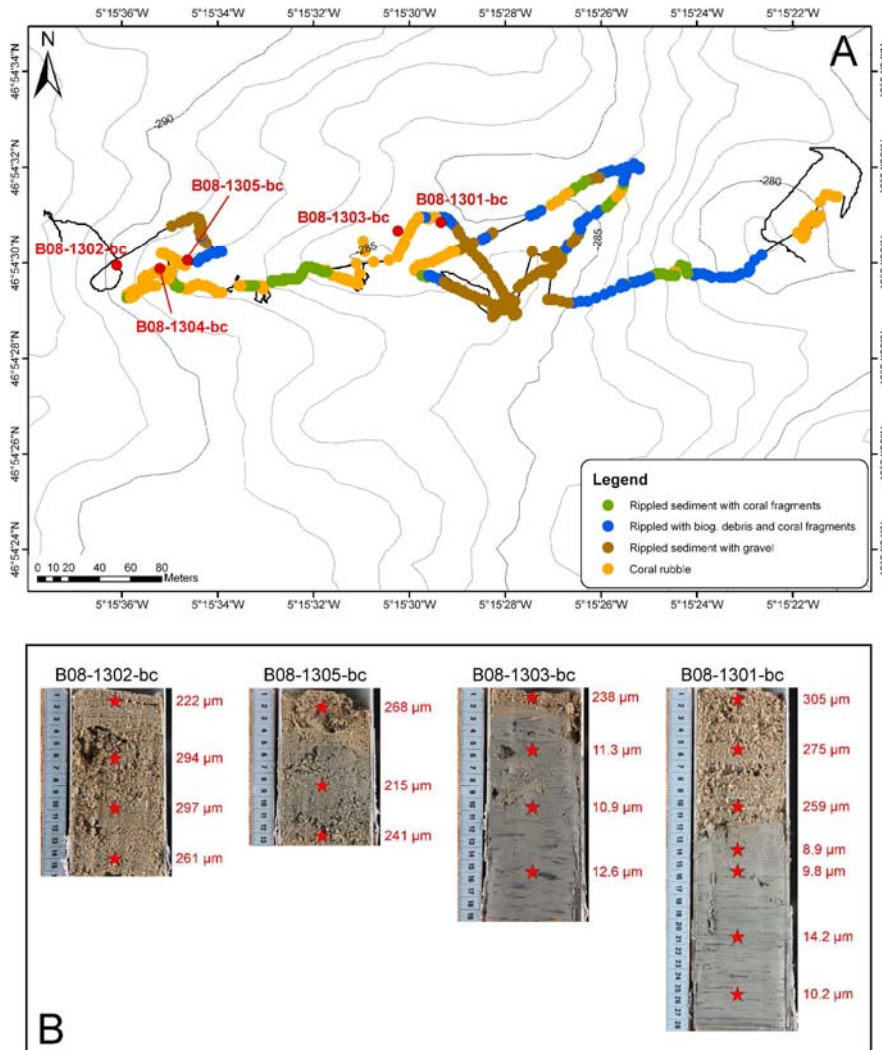


865

866 ROV images from the shallow-water setting (ROV dive B08-03): (A) rippled seabed
867 with a patchy distribution of cold-water corals, (B) coarse sand with a high amount of
868 gravel, (C) the dense cold-water coral rubble coverage on top of the small mounds, and
869 (D) zoom in this coral rubble facies with predominantly *Lophelia pertusa*.

870

871 Figure 4.



872

873 (A) Facies interpretation map of the shallow-water dive B08-03 on the southeastern

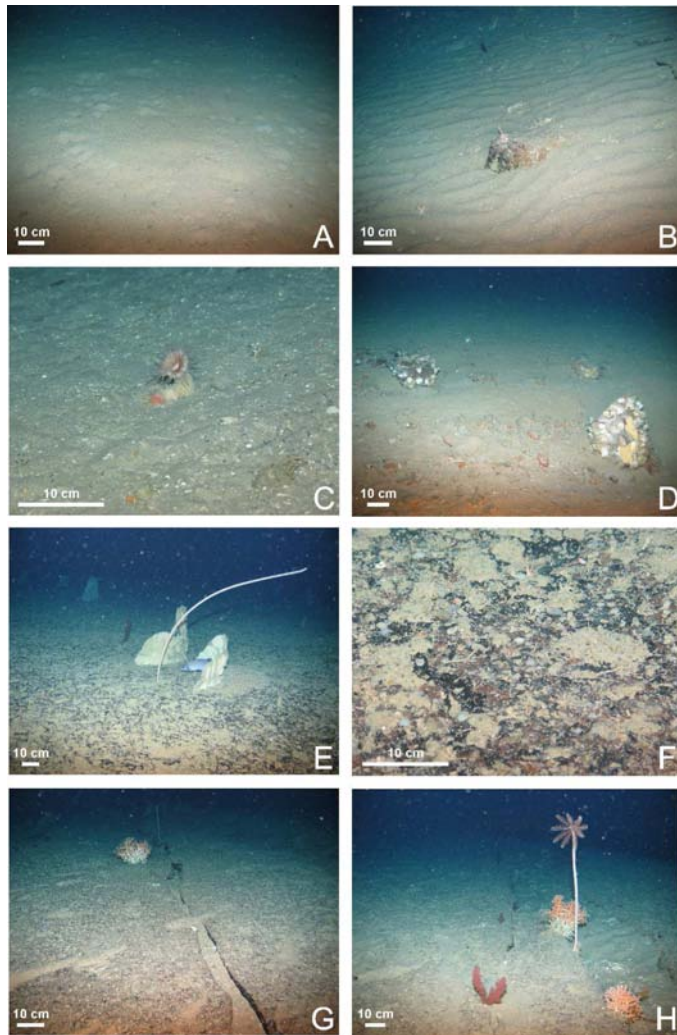
874 flank of the Guilvinec Canyon in water depths between 278 and 289 m. (B) Photographs

875 of the obtained boxcores in the shallow water area with the locations and mean grain-

876 size values.

877

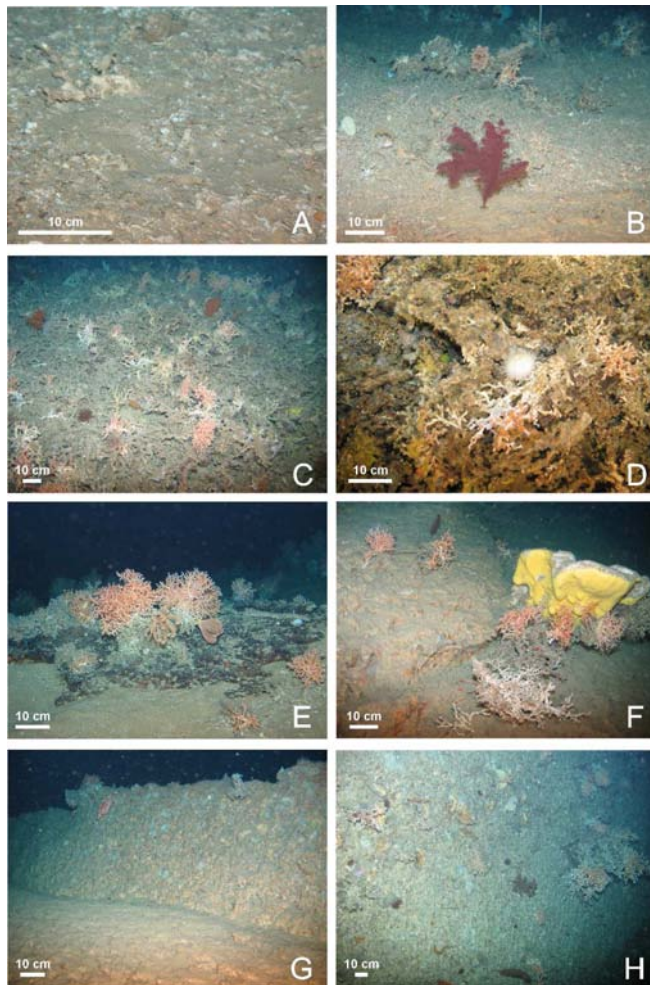
878 Figure 5.



879

880 ROV stills imagery highlighting the most important facies and associated fauna in the
881 deep-water setting: (A) soft sediment with bioturbations; (B) rippled soft sediment with
882 gravel; (C) a seabed covered with biogenic debris; (D) soft sediment with a patchy
883 distribution of gravel; (E) hard substrate with a patchy distribution of cold-water corals,
884 sponges and a sea urchin; (F) zoom on the hard substrate; (G) hard substrate with a
885 large crack and one *Madrepora oculata* species; (H) hard substrate with a crack filled
886 up with rippled soft sediment, colonised by a crinoid and a few living *Madrepora*
887 *oculata* corals.

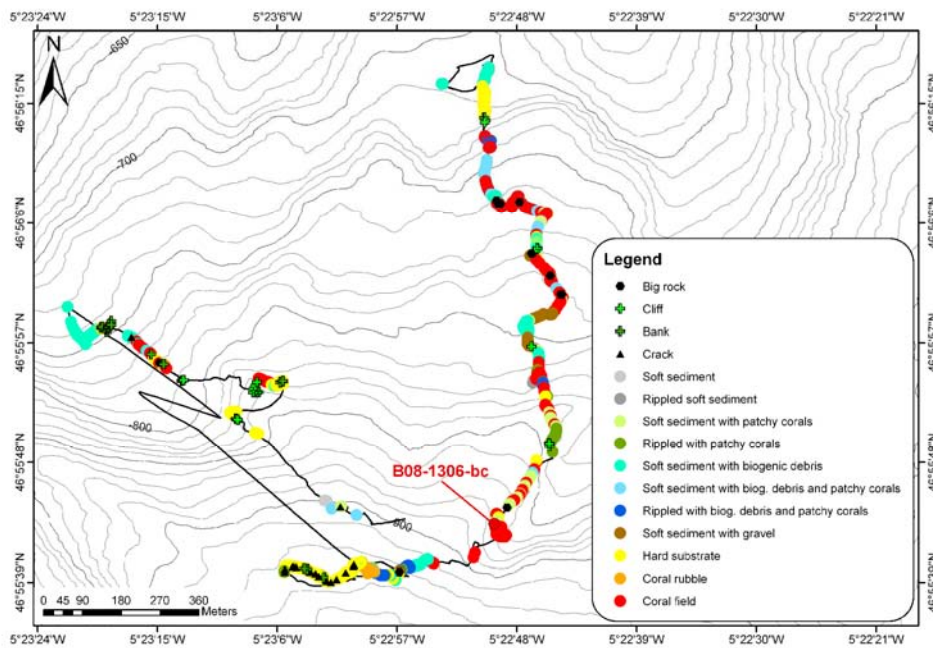
888 Figure 6.



889

890 ROV stills imagery highlighting the different types of cold-water coral occurrences in
891 the deep-water coral setting: (A) rippled seabed with coral rubble and biogenic debris;
892 (B) example of a coral field with living and dead coral species; (C) a dense cold-water
893 coral coverage with both living and dead species; (D) detailed zoom on the facies
894 mentioned in A; (E) outcropping hard substratum with a few living coral species
895 (*Madrepora oculata*) and Gorgonians; (F) outcropping hard substratum with the
896 sponges *Geodia sp.* and *Topsentia sp.*, and again living and dead *Madrepora oculata*
897 specimens; (G) a small bank with a height of 50 cm colonised by oysters and a few
898 living coral species; (H) a vertical cliff colonised with oysters and living *Madrepora*
899 *oculata*.

900 Figure 7.



901

902 Facies interpretation map of ROV dive B08-02 on the northwestern flank of the

903 Guilvinec Canyon in water depths of 712 to 900 m.

904

905 **Tables**

906

907 Table 1. Names, locations and operational data of the ROV Genesis dives. Time in

908 UTC.

Name	Area	Start track		End track	
		Time	Depth	Time	Depth
B08-01	South flank of Penmarc'h canyon	13:16:02	385 m	16:47:44	699 m
B08-02	North flank of Guilvinec canyon	11:24:46	712 m	15:46:00	900 m
B08-03	South flank of Guilvinec canyon: small mounds/ridges on the top	12:29:41	278 m	14:05:25	289 m
B08-04	Spur, south flank of Guilvinec canyon	15:51:10	676 m	16:38:51	691 m
B08-05	North flank of Guilvinec canyon	11:17:00	305 m	14:27:53	529 m

909

910

911 Table 2. Location, water depth and recovery length of the studied boxcores.

Core number	Latitude	Longitude	Water Depth	Recovery
B08-1301-bc	46°54.514' N	5°15.489' W	285 m	31 cm
B08-1302-bc	46°54.499' N	5°15.602' W	290 m	17 cm
B08-1303-bc	46°54.511' N	5°15.504' W	285 m	20 cm
B08-1304-bc	46°54.498' N	5°15.587' W	288 m	5 cm
B08-1305-bc	46°54.501' N	5°15.577' W	288 m	14 cm
B08-1306-bc	46°55.723' N	5°22.828' W	866 m	10-15 cm

912

913 Table 3. Overview of the U-series datings in the shallow water setting (left) and the
 914 deep-water setting (right).

Shallow water setting			Deep-water setting		
Sample name	Age (ka)	Error (ka)	Sample name	Age (ka)	Error (ka)
B08-1301-bc	7.35	0.45	B08-1306-bc A	1.32	0.52
B08-1305-bc A	7.78	0.71	B08-1306-bc B	1.21	0.13
B08-1305-bc A	9.07	0.25	B08-1306-bc C	2.27	0.30
B08-03 B	8.89	0.31			
B08-03 C	1.41	0.17			

915